Supporting Information

Breathable, recyclable, and solvent-free conductive films: versatile processing for flexible biointerfaces

Yi Qian,[a] Yuyu Zhang,[a] Jinhao Huang,[a] Qiongya Li,[b] Fusheng Zhang*[ab] and Guangyan Qing*[ab]

[a] Hubei Key Laboratory of Biomass Fibers and Eco-dyeing & Finishing, College of Chemistry and Chemical Engineering, Wuhan Textile University, Wuhan 430200 P. R. China
[b] CAS Key Laboratory of Separation Science for Analytical Chemistry, Dalian Institute of Chemical Physics, Chinese Academy of Sciences, Dalian 116023, P. R. China

E-mail: fszhang@wtu.edu.cn, qinggy@dicp.ac.cn

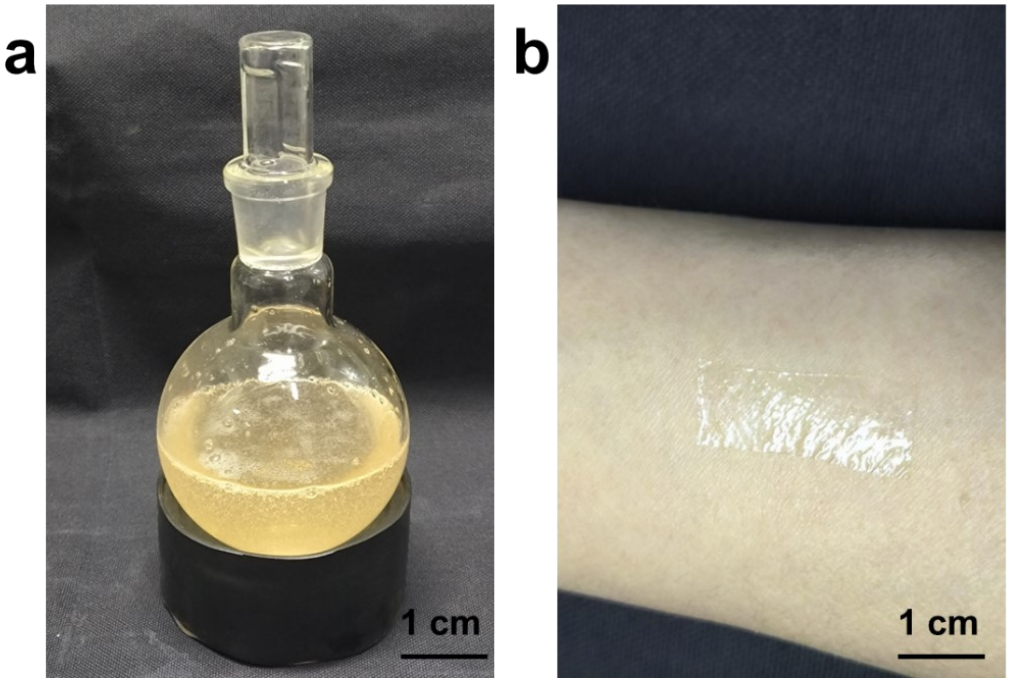

Figure S1. Images of precursor SIB ink (a) and SIB film on the human skin (b).

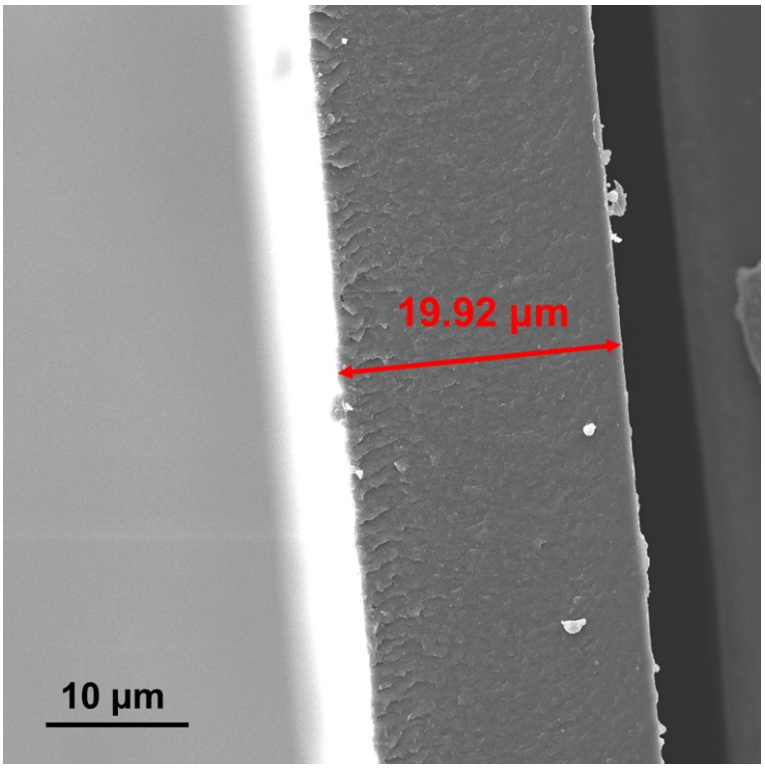

Figure S2. Cross-section SEM image of the SIB-2 film.

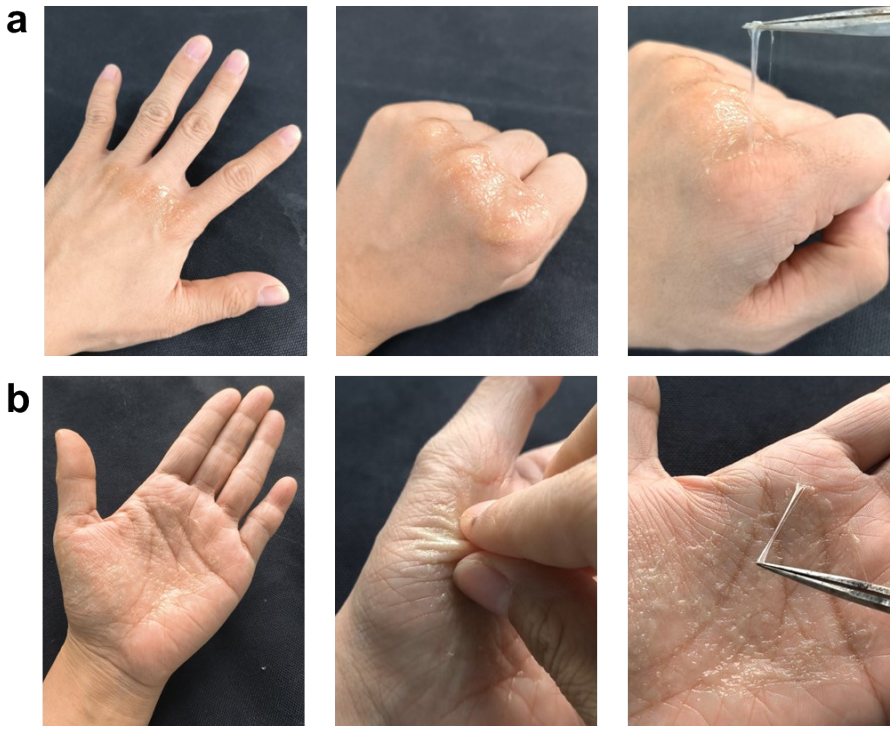

Figure S3. Applying SIB ink to the finger joint (a) or palm (b) allows for the rapid formation of films with adaptive adhesion.

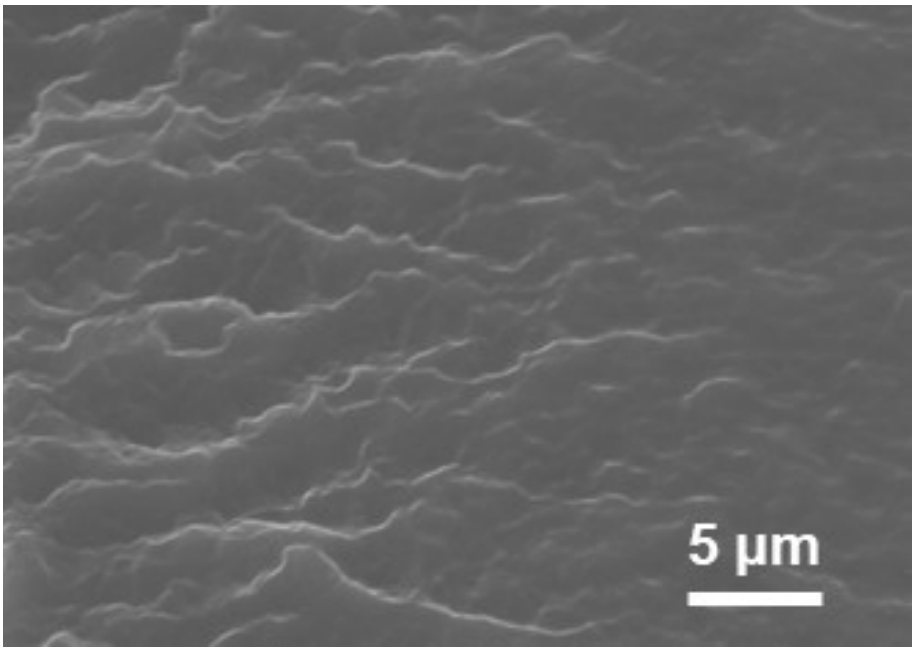

Figure S4. Cross-section SEM image of the SIB-2 film at high magnification.

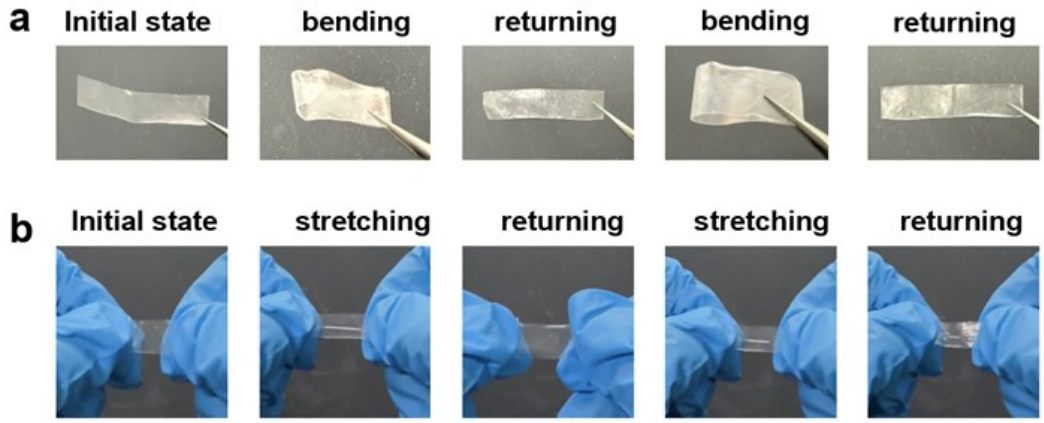

Figure S5. The repeated bending (a) and stretching tests (b) of the SIB-2 film.

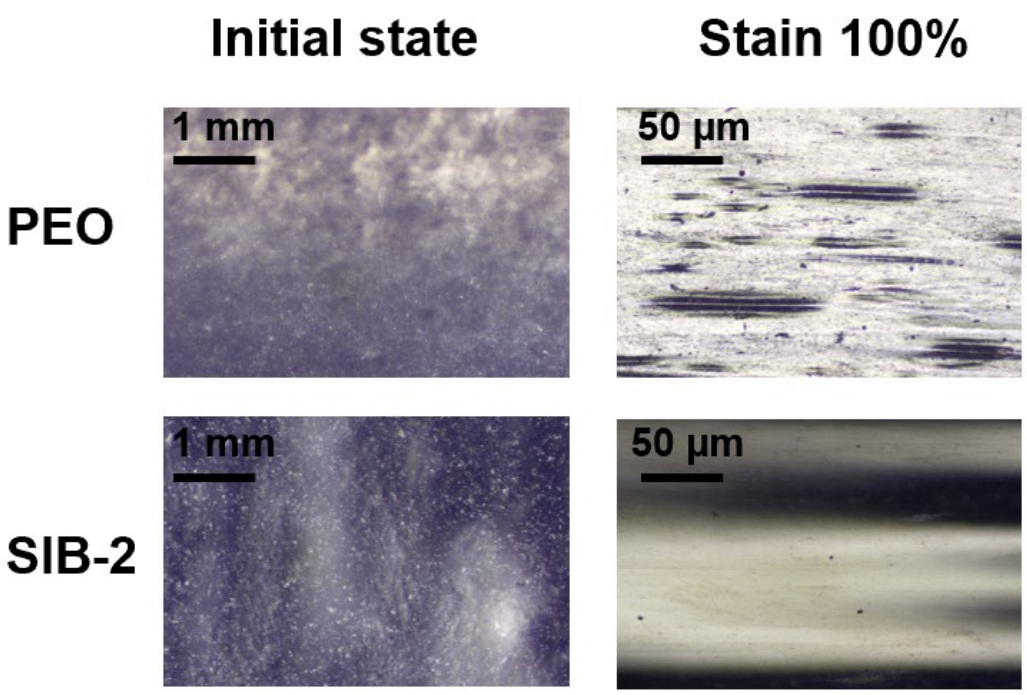

Figure S6. Comparison of initial state and 100% stretching images of pure PEO film and SIB-2 film.

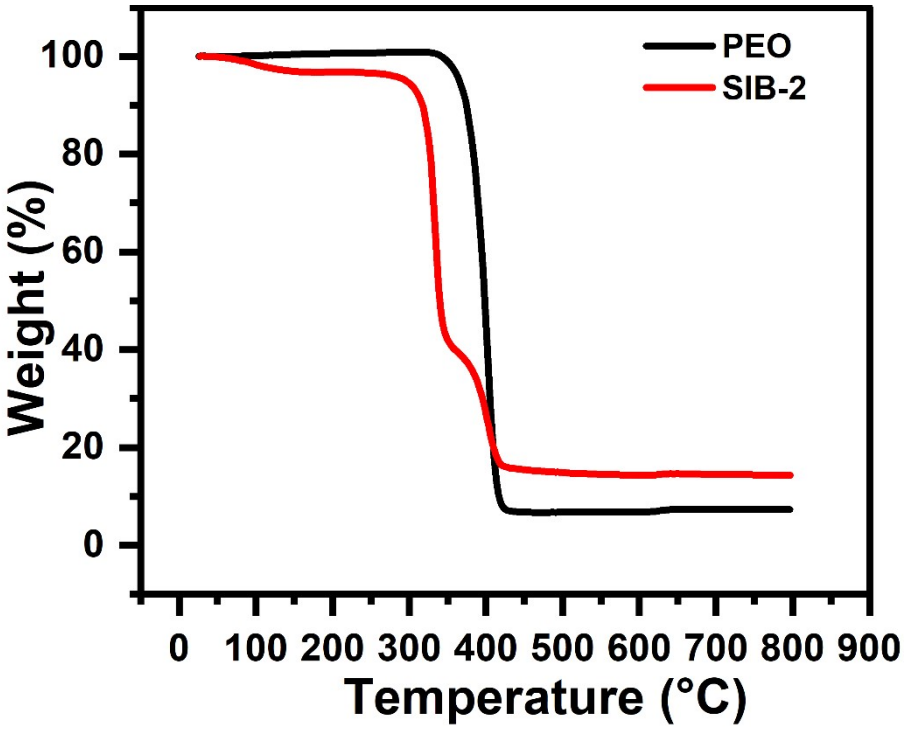

Figure S7. TGA curves for pure PEO film and SIB-2 film.

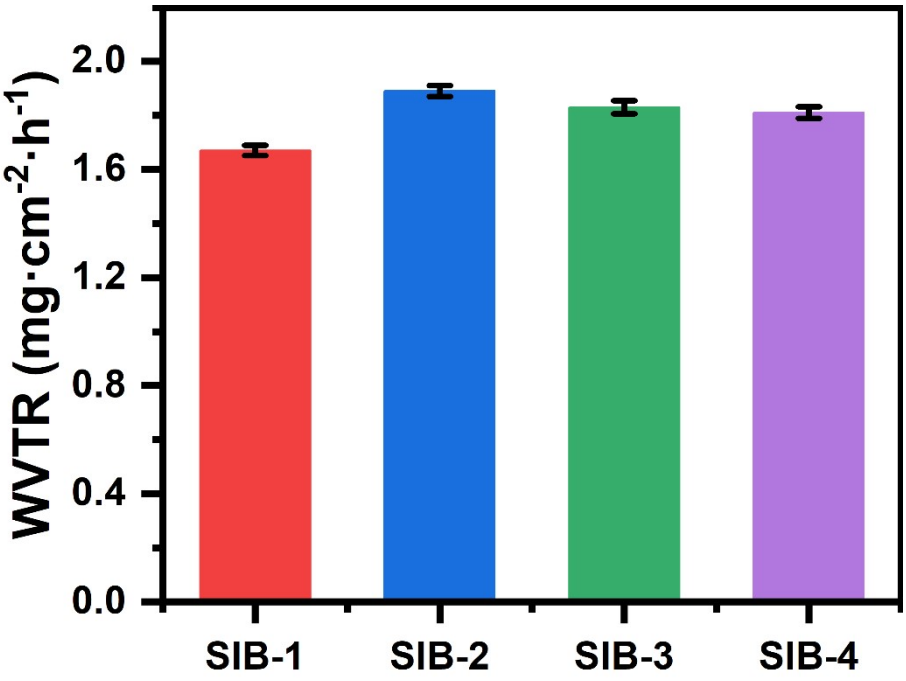

Figure S8. The WVTR of the pure PEO film and different SIB films.

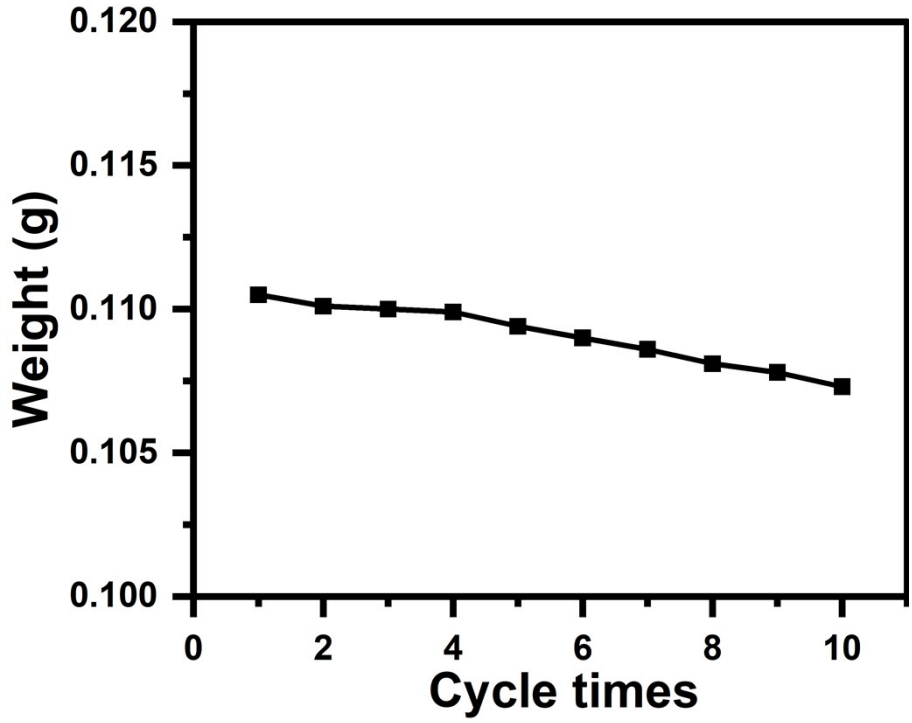

Figure S9. Weight measurements of the SIB-2 film after cycling from one to ten times.

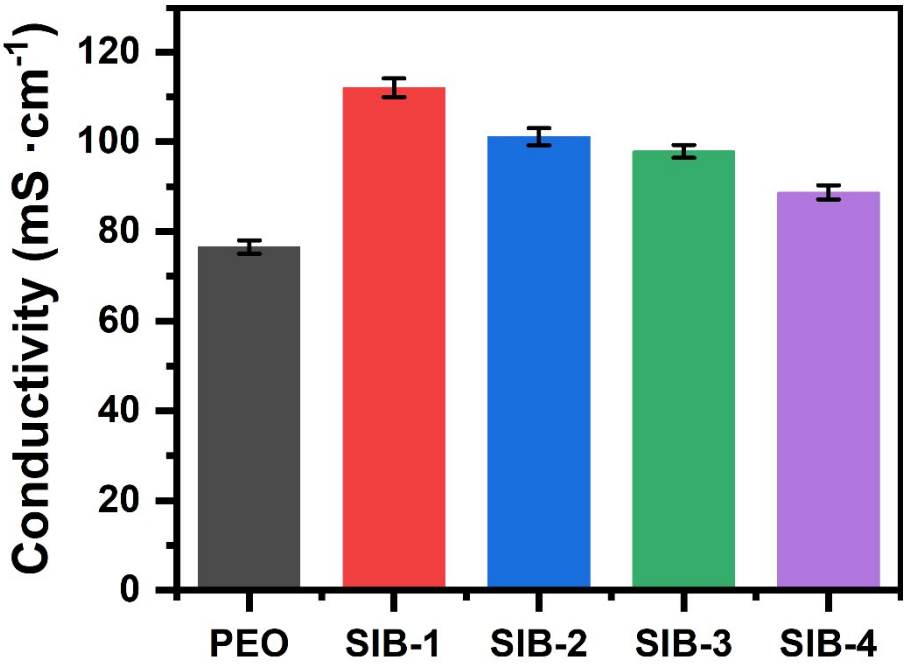

Figure S10. Conductivity of the pure PEO film and different SIB films.

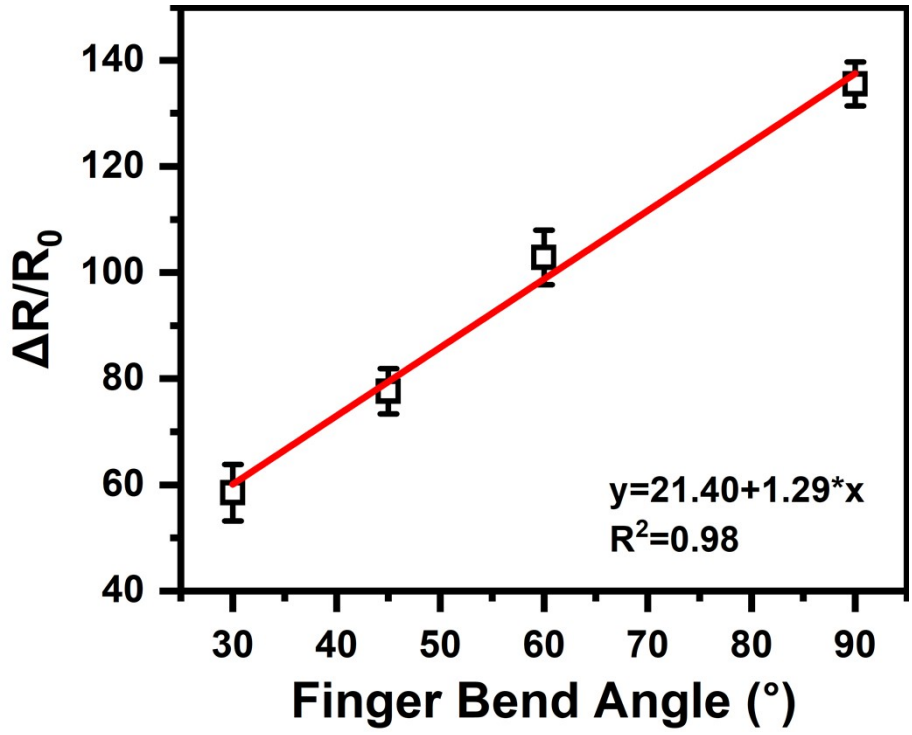

Figure S11. Relationship between $\Delta R/R_0$ and the finger bend angle of the SIB-1 film.

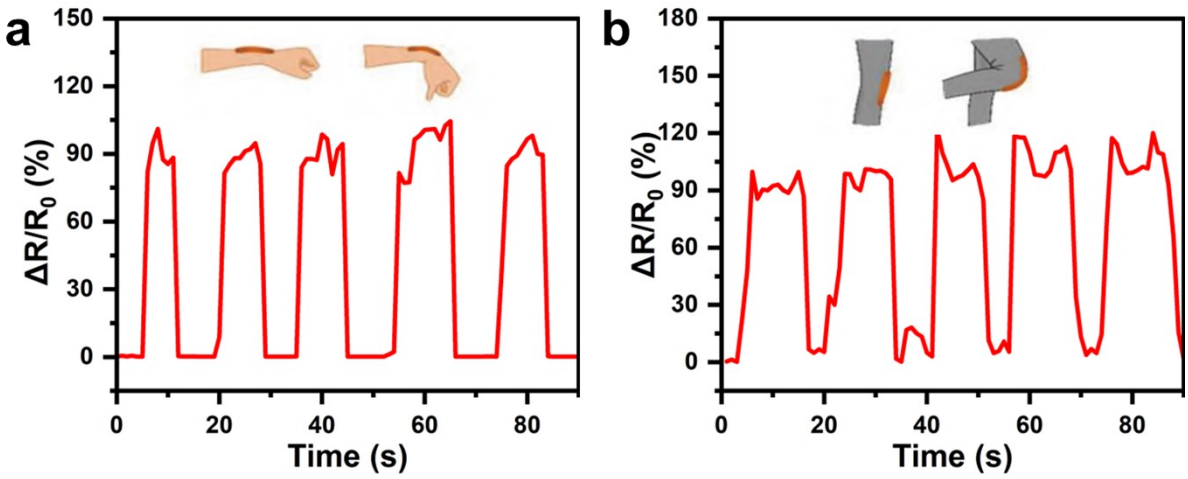

Figure S12. Relative resistance change curves of the SIB-1 film during repeated bending of the wrist (a) and knee (b).

Figure S13. Photograph of a leaf covered with the SIB-1 film after 7 days.

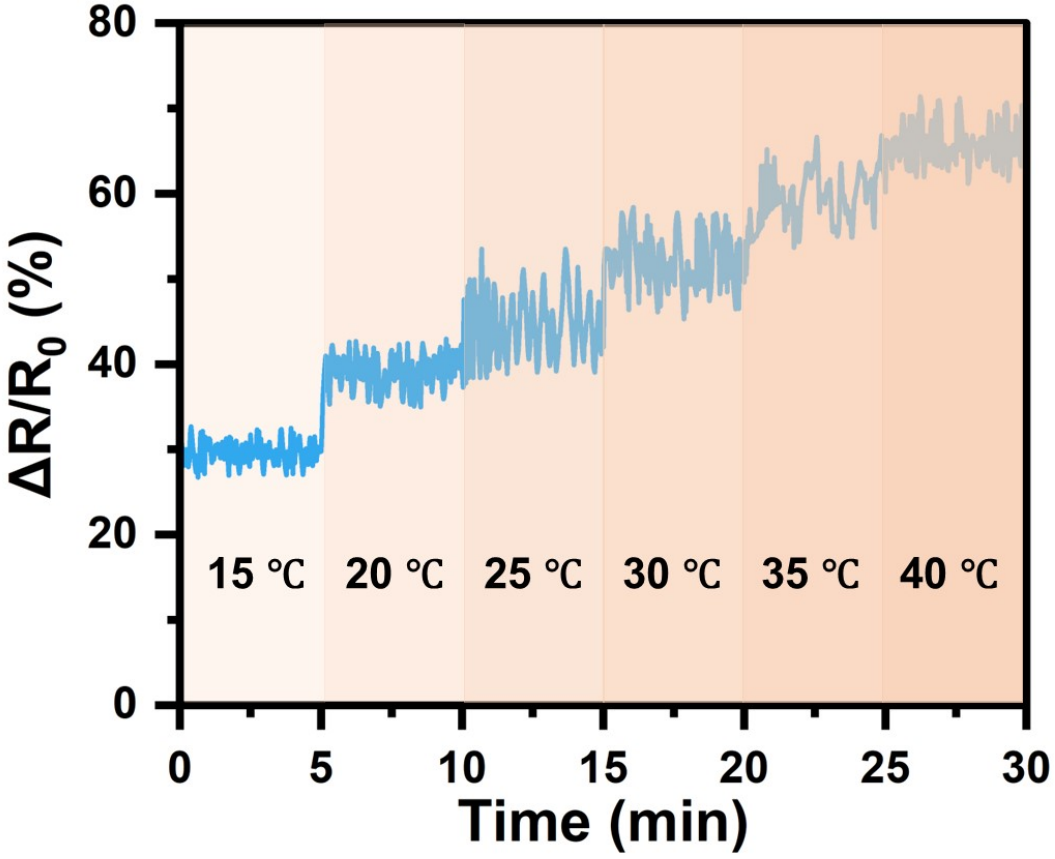

Figure S14. Relative resistance change curves of the SIB-1 film at different temperatures.

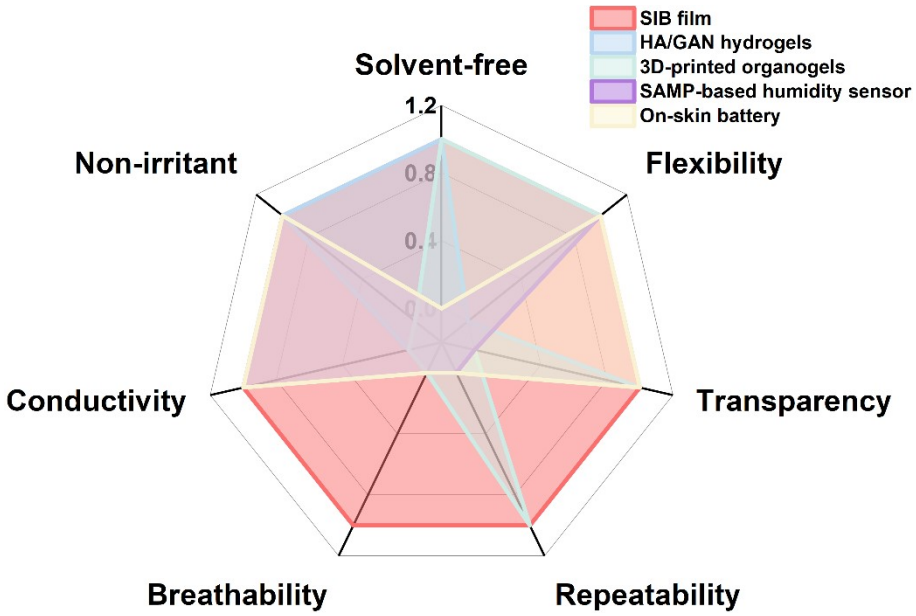

Figure S15. Comparison of comprehensive performance of biological interface materials.[1-4]

Table S1. Comparison of water vapour transmission rate (WVTR) with similar materials reported in the literature.

Name of materials	WVTR ($mg \cdot cm^{-2} \cdot h^{-1}$)
SIB-2 film	1.89
PDMS	0.03
CE	0.04
CBPFB	0.0688
Parylene	0.0690
BNC	0.08875
3M Tegater	0.5
HP band	1.0458

Table S2. Comparison of comprehensive performance of biological interface materials.[1-4]

Name of Materials	Solvent-free	Flexibility	Transparency	Repeatability	Breathability	Conductivity	Non-irritant
SIB film	√	√	√	√	√	√	√
HA/GAN hydrogels[1]	√	×	√	×	×	×	√
3D-printed organogels[2]	√	√	×	√	×	×	×
SAMP-based humidity sensor[3]	×	√	×	×	×	√	√
On-skin battery[4]	×	√	√	×	×	√	√

Reference

1 E. Larrañeta, M. Henry, N. J. Irwin, J. Trotter, A. A. Perminova and R. F. Donnelly, *Carbohydrate Polymers*, 2018, **181**, 1194–1205.

2 M. A. Kuzina, M. Hoffmann, N. K. Mandsberg, C. M. Domínguez, C. M. Niemeyer, M. Wilhelm and P. A. Levkin, *Advanced Functional Materials*, 2024, **34**, 2403694.

3 T. Li, T. Zhao, H. Zhang, L. Yuan, C. Cheng, J. Dai, L. Xue, J. Zhou, H. Liu, L. Yin and J. Zhang, *npj Flex Electron*, 2024, **8**, 1–9.

4 L. Gao, Z. Wang, Y. Zen, Y. Wang, Q. Ren, Z. Ding, K. Ni, J. Tang, C. Zhang, Y. Wang, Y. Zhou, J. Hui, Q. Lu, R. Liu and X. Zhang, *Advanced Functional Materials*, 2024, **34**, 2410140.